REFERENCES

1. D. Schurig, J.B. Pendry, and D.R. Smith, Calculation of material properties and ray tracing in transformation media, Opt Express 14 (2006), 9794–9804.
2. U. Leonhardt and T.G. Philbin, General relativity in electrical engineering, New J Phys 8 (2006), 247.
3. U. Leonhardt, Optical conformal mapping, Science 312 (2006), 1777–1780.
4. D. Schurig, J.J. Mock, B.J. Justice, S.A. Cummer, J.B. Pendry, A.F. Starr, and D.R. Smith, Metamaterial electromagnetic cloak at microwave frequencies, Science 314 (2006), 977–980.
5. A. Greenleaf, Y. Kurylev, M. Lassas, and G. Uhlmann, Electromagnetic wormholes and virtual magnetic monopoles from metamaterials, Phys Rev Lett 99 (2007), 183901.
6. M. Rahm, D. Schurig, D.A. Roberts, S.A. Cummer, D. R. Smith, and J.B. Pendry, Design of electromagnetic cloaks and concentrators using form-invariant coordinate transformations of Maxwell's equations, Photon Nanostruct – Fundam Appl 6 (2008), 87–95.
7. A.D. Yaghjian and S. Maci, Alternative derivation of electromagnetic cloaks and concentrators, in press; arXiv:0710.2933v4 [physics.class-ph].
8. H.Y. Chen and C.T. Chan, Transformation media that rotate electromagnetic fields, Appl Phys Lett 90 (2007), 241105.
9. Y. Luo, J. Zhang, L. Ran, H. Chen, and J.A. Kong, Controlling the emission of electromagnetic sources by coordinate transformation, in press; arXiv:0712.3776v1 [physics.optics].
10. D. Schurig, J.B. Pendry, and D.R. Smith, Transformation-designed optical elements, Opt Express 15 (2007), 14772–14782.
11. A.V. Kildishev and E.E. Narimanov, Impedance-matched hyperlens, in press; arXiv:0708.3798v1 [physics.optics].
12. M. Tsang and D. Psaltis, Magnifying perfect lens and superlens design by coordinate transformation, Phys Rev B 77 (2008), 035122.
13. A.V. Kildishev and V.M. Shalaev, Engineering space for light via transformation optics, Opt Lett 33 (2008), 43–45.
14. J.B. Pendry, D. Schurig, and D.R. Smith, Controlling electromagnetic fields, Science 312 (2006), 1780–1782.
15. P.-S. Kildal, A. Kishk, and A. Tengs, Reduction of forward scattering from cylindrical objects using hard surfaces, IEEE Trans Antennas Propagat 44 (1996), 1509–1520.
16. D.A.B. Miller, On perfect cloaking, Opt Express 14 (2006), 12457–12466.
17. A. Alù and N. Engheta, Plasmonic materials in transparency and cloaking problems: Mechanism, robustness, and physical insights, Opt Express 15 (2007), 3318–3332.
18. Y. Huang, Y. Feng, and T. Jiang, Electromagnetic cloaking by layered structure of homogeneous isotropic materials, Opt Express 15 (2007), 11133–11141.
19. A. Hakansson, Cloaking of objects from electromagnetic fields by inverse design of scattering optical elements, Opt Express 15 (2007), 4328–4334.
20. M.G. Silveirinha, A. Alù, and N. Engheta, Parallel-plate metamaterials for cloaking structures, Phys Rev E 75 (2007), 036603.
21. N.A.P. Nicorovici, G.W. Milton, R.C. McPhedran, and L.C. Botten, Quasistatic cloaking of two-dimensional polarizable discrete systems by anomalous resonance, Opt Express 15 (2007), 6314–6323.
22. P. Alitalo, O. Luukkonen, L. Jylha, J. Venermo, and S.A. Tretyakov, Transmission-line networks cloaking objects from electromagnetic fields, IEEE Trans Antennas Propagat 56 (2008), 416–424.
23. H.S. Chen, B.I. Wu, B. Zhang, and J.A. Kong, Electromagnetic wave interactions with a metamaterial cloak, Phys Rev Lett 99 (2007), 063903.
24. B. Zhang, H.S. Chen, B.I. Wu, Y. Luo, L.X. Ran, and J.A. Kong, Response of a cylindrical invisibility cloak to electromagnetic waves, Phys Rev B 76 (2007), 121101.
25. Z. Ruan, M. Yan, C.W. Neff, and M. Qiu, Ideal cylindrical cloak: Perfect but sensitive to tiny perturbations, Phys Rev Lett 99 (2007), 113903.
26. M. Yan, Z.C. Ruan, and M. Qiu, Cylindrical invisibility cloak with simplified material parameters is inherently visible, Phys Rev Lett 99 (2007), 233901.
27. H.Y. Chen, Z.X. Liang, P.J. Yao, X.Y. Jiang, H.R. Ma, and C.T. Chan, Extending the bandwidth of electromagnetic cloaks, Phys Rev B 76 (2007), 241104.
28. W.S. Cai, U.K. Chettiar, A.V. Kildishev, and V.M. Shalaev, Optical cloaking with metamaterials, Nat Photon 1 (2007), 224–227.
29. W. Cai, U.K. Chettiar, A.V. Kildishev, V.M. Shalaev, and G.W. Milton, Nonmagnetic cloak with minimized scattering, Appl Phys Lett 91 (2007), 111105.
30. COMSOL Multiphysics—User's Guide, COMSOL AB, 2005.
31. M. Abramowitz and I.A. Stegun, Handbook of mathematical functions, Dover, New York, NY, 1964.
32. O.M. Bucci and G. Franceschetti, On the degrees of freedom of scattered fields, IEEE Trans Antennas Propagat 37 (1989), 918–926.

EXPERIMENTAL VALIDATION OF PERCOLATION-BASED MODELS FOR PROPAGATION PREDICTION

R. Azaro, A. Martini, and A. Massa
ELEDIA Research Group Department of Information and Communication Technology University of Trento, Via Sommarive 14, I-38050 Trento, Italy; Corresponding author: andrea.massa@ing.unitn.it

Received 12 April 2008

ABSTRACT: *In this letter, an experimental validation of percolation-based approaches for the prediction of wave propagation in random media is presented. Measurements are collected in a real controlled environment, where the obstacles are stochastically placed in a two-dimensional grid according to a known nonuniform density distribution. The obtained results show that, in spite of their simplicity, percolation-based approaches can be applied in real propagation problems.* © 2008 Wiley Periodicals, Inc. Microwave Opt Technol Lett 50: 3190–3192, 2008; Published online in Wiley InterScience (www.interscience.wiley.com). DOI 10.1002/mop.23937

Key words: *percolation theory propagation; stratified random media; electromagnetic propagation; experimental validation*

1. INTRODUCTION

The prediction of e.m. propagation in disordered distributions of obstacles is a challenging research topic [1]. A possible approach to such a topic consists of modeling the propagation environment by means of a percolation lattice [2] and describing the propagation through a stochastic process. This allows one to obtain analytical closed-form solutions that describe the average properties of the e.m. propagation [3, 4]. With reference to the far-external source scenario and under the assumption that the obstacles are nonuniformly distributed, this letter is aimed at presenting the results of an experimental validation performed in a real controlled environment to validate the percolation-based solutions [5, 6].

2. SETUP

The experiments have been carried out in an anechoic chamber, 6 m long, 3 m wide, and 4 m high, available at the ELEDIA laboratory. Sketch and wide-angle shot of the experimental setup are given in Figures 1 and 2, respectively. A 2 m-sided square area has been partitioned in $K = 10$ rows, each one containing $I = 10$ cells. Obstacle were polystyrene cylinders with square section (0.2 m $\times$ 0.2 m), 2 m high, lined with a metallic film. The transmitting device, aimed at modeling the e.m. source, was an Oritel ANC 100/15 dB pyramidal horn antenna whose dimensions have been

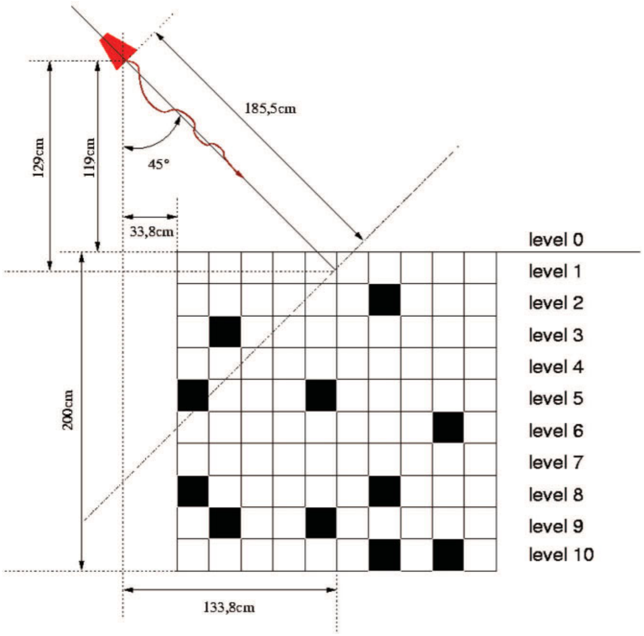

Figure 1 Sketch of the experimental setup. [Color figure can be viewed in the online issue, which is available at www.interscience.wiley.com]

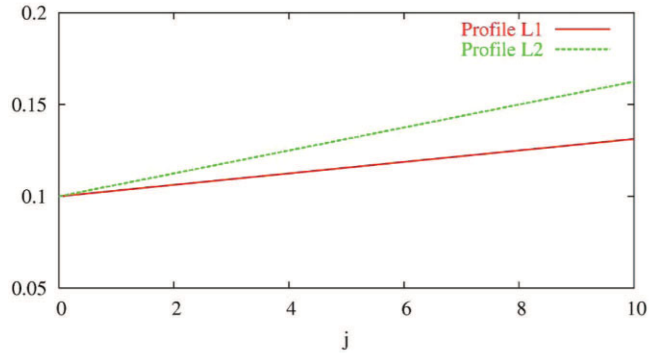

Figure 3 Obstacles density profiles. [Color figure can be viewed in the online issue, which is available at www.interscience.wiley.com]

increased by means of metallic plates to 190 mm, 130 mm, and 120 mm, respectively. The transmitting antenna has been placed in the crosssectional plane of the targets, and it has been oriented so that its symmetry axis crosses the middle of the first row and forms an angle of 45° with the upper side of the grid (see Fig. 1). The working frequency has been set to 9.6 GHz. As both the transmitting antenna and the receiving one (i.e., a vertical half-wavelength monopole connected to an Agilent E4407B network analyzer) are fixed at a height equal to the half of the scatterers height, the behavior in the horizontal plane quite carefully approximate a two-dimensional scenario. The experiments are concerned with two linear obstacles density distributions (namely, Profile L1 and Profile L2 in Fig. 3) where the occupancy probability takes the form $q_j = q_1 + \alpha j$, j being the row index. For each obstacles density profile, $S = 20$ different grid realizations (referred in the following as maps and randomly generated according to the chosen profile distribution) have been considered. For each map, experimental data have been collected by locating the scatterers one row after the other. The measurements have been collected in the successive and adjacent row by moving the dipole in correspondence with each one of the $I = 10$ columns.

Definitions: The measured average path loss at a given row k is equal to:

$$\langle \mathrm{PL}(k) \rangle^{\mathrm{meas}} = -10 \log_{10}\left[\frac{1}{P_{\mathrm{T}}}\left(\frac{1}{IS}\sum_{i=1}^{I}\sum_{s=1}^{S} P_{\mathrm{R}}^{\mathrm{m}}[(k,i);s]\right)\right][\mathrm{dB}] \quad (1)$$

where P_{T} is the transmitted power, and $P_{\mathrm{R}}^{\mathrm{m}}[(k,i);S]$ is the power measured at the $(k+1,i)$-th site in correspondence with the sth realization when the grid is filled with obstacles till level k. On the other hand, the same quantity is numerically estimated according to the following relationship:

$$\langle \mathrm{PL}(k) \rangle = -10 \log_{10}\left[\frac{\langle P_{\mathrm{R}}^{\mathrm{fs}}(k)\rangle \Pr\{0 \rightarrow k\}}{P_{\mathrm{T}}}\right][\mathrm{dB}] \quad (2)$$

where $\langle P_{\mathrm{R}}^{\mathrm{fs}}(k)\rangle$ is the average power received at level k in free space, and $\Pr\{0 \rightarrow k\}$ is the probability that a single ray impinging on the two-dimensional percolation lattice reaches level k before being reflected back into the above empty halfplane. Such quantity is analytically computed by following either the Markov approach [5] or the Martingale approach [6].

3. RESULTS

Figures 4 and 5 show the results obtained for the obstacles density profiles in Figure 3 by means of (2) by applying the Martingale as well as the Markov approach. The estimated values are compared with those measured and using (1). Although several sources of error as well as approximations (e.g., measurement inaccuracies,

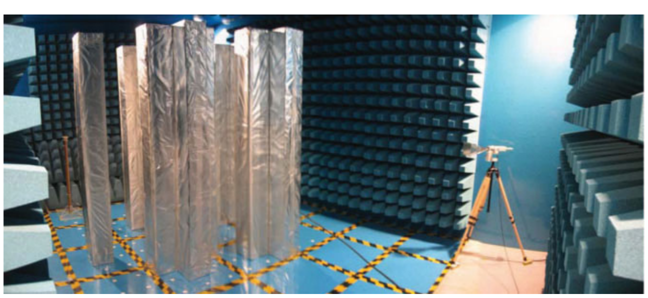

Figure 2 Wide-angle shot of the experimental setup. [Color figure can be viewed in the online issue, which is available at www.interscience.wiley.com]

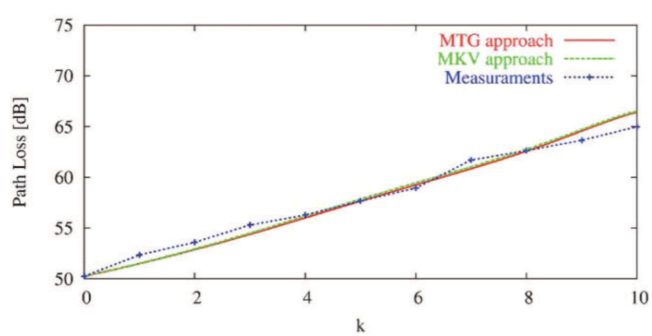

Figure 4 Estimated and reference values of $\langle \mathrm{PL}(k) \rangle$ vs. k for the Profile L1. [Color figure can be viewed in the online issue, which is available at www.interscience.wiley.com]

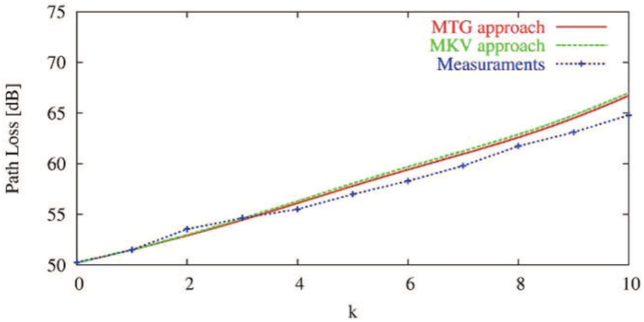

Figure 5 Estimated and reference values of ⟨PL(*k*)⟩ vs. *k* for the Profile L2. [Color figure can be viewed in the online issue, which is available at www.interscience.wiley.com]

not infinite grid in the horizontal direction, not perfect two-dimensional structure, limited data sample) are present, a good matching between theoretical and reference data can be noticed whatever the obstacles distribution and the prediction approach.

4. CONCLUSIONS

In this letter, some representative results from an experimental validation of percolation-based approaches for the prediction of wave propagation in random media have been presented. The matching between measured and computed data values has assessed the reliability of statistic strategies.

REFERENCES

1. A. Ishimaru, Wave propagation and scattering in random media, IEEE Press, New York, NY, 1997.
2. G. Grimmet, Percolation, Springer-Verlag, Berlin, Germany, 1989.
3. G. Franceschetti, S. Marano, and F. Palmieri, Wave propagation without wave equation towards an urban area model, IEEE Trans Antennas Propagat (47) 1999, 1393–1404.
4. S. Marano and M. Franceschetti, Ray propagation in a random lattice, a maximum entropy anomalous diffusion process, IEEE Trans Antennas Propagat (53) 2005, 1888–1896.
5. A. Martini, M. Franceschetti, and A. Massa, Ray propagation in nonuniform random lattices, J Opt Soc Am A (23) 2006, 2251–2261.
6. A. Martini, R. Azaro, M. Franceschetti, and A. Massa, Ray propagation in nonuniform random lattices-part II, J Opt Soc Am A (24) 2007, 2363–2371.

GSM850/900/1800/1900/UMTS PRINTED MONOPOLE ANTENNA FOR MOBILE PHONE APPLICATION

Kin-Lu Wong and Ting-Wei Kang
Department of Electrical Engineering, National Sun Yat-Sen University, Kaohsiung 80424, Taiwan; Corresponding author: kangtw@ema.ee.nsysu.edu.tw

Received 13 April 2008

ABSTRACT: *The design of a printed monopole antenna on the system circuit board of the mobile phone for achieving GSM850/900/1800/1900/UMTS operation with a small area of 10 mm × 60 mm is presented. The antenna is easy to fabricate at low cost and mainly comprises a driven strip, a coupled strip, and a high-pass matching network for providing two wide operating bands at about 900 and 1900 MHz to cover GSM850/900 and GSM1800/1900/UMTS operations, respectively. The wide lower band is controlled by the driven strip excited as a quarter-wavelength mode, which is further tuned to become a dual-resonance excitation by incorporating the high-pass matching network for effective bandwidth enhancement. For the wide upper band, it is formed by a quarter-wavelength mode excited at about 1800 MHz by the coupled strip and the higher-order mode contributed by the driven strip. Furthermore, with the proposed antenna structure, the lower and upper bands can generally be tuned separately, which is an attractive feature and makes it easy to design for practical applications.* © 2008 Wiley Periodicals, Inc. Microwave Opt Technol Lett 50: 3192–3198, 2008; Published online in Wiley InterScience (www.interscience.wiley.com). DOI 10.1002/mop.23936

Key words: *mobile antennas; printed monopole antennas; mobile phone antennas; multiband antennas; penta-band operation*

1. INTRODUCTION

Owing to the rapid growth in mobile communications, the internal antenna for the mobile phone is generally required to be capable of multiband operation, especially penta-band operation covering GSM850/900/1800/1900/UMTS (824∼894/890∼960/1710∼1880/1850∼1990/1920∼2170 MHz) operation. However, owing to the limited space available inside the mobile phone, it is usually a big challenge for antenna engineers to achieve penta-bend operation for the internal mobile phone antenna with a small size.

In this article, we present a promising design of using a printed monopole antenna to achieve penta-band operation for the mobile phone. The proposed printed monopole antenna is to be printed directly on the system circuit board of the mobile phone, hence making it easy to fabricate at low cost. In addition, the printed monopole antenna is of low profile in appearance and, thus, especially suitable for application in a thin mobile phone [1–4]. The proposed antenna also provides a promising solution for the printed monopole for internal mobile phone antenna applications to easily generate two wide operating bands for covering GSM850/900 and GSM1800/1900/UMTS operations. The proposed printed monopole shows a simple radiating metal pattern of a driven strip and a coupled strip. The enhanced bandwidth in the lower band at about 900 MHz is obtained by incorporating a high-pass matching network [5–10] to the printed monopole, which results in a dual-resonance excitation for the excited resonant mode in the lower band; this leads to a wide lower band for the antenna to cover GSM850/900 operation. On the other hand, the coupled strip can contribute an additional resonant mode for the antenna's upper band to achieve a much widened bandwidth to cover GSM1800/1900/UMTS operation. In addition, as the coupled strip is excited through a small coupling gap by the driven strip [11], not through direct excitation as the traditional two-branch monopole antenna [12–14], its effect on the existing resonant modes contributed by the driven strip are found to be very small. This behavior makes the lower and upper bands of the proposed monopole antenna easy to be adjusted separately. This makes the antenna easy to design for practical applications. Details of the proposed printed monopole antenna for penta-band operation are presented.

2. DESIGN OF PROPOSED PRINTED MONOPOLE ANTENNA

Figure 1(a) shows the geometry of the proposed printed monopole antenna for GSM850/900/1800/1900/UMTS operation in the mobile phone, and the equivalent circuit of the high-pass matching network incorporated to the antenna is shown in Figure 1(b). The printed monopole consists of a driven strip and a coupled strip; both strips are in a folded configuration to achieve a compact size. The driven and coupled strips are printed on the small top no-